



Transport Properties of Ethane, Butanes and Their Binary Mixtures in MFI-Type Zeolite and Zeolite-Membrane Samples

MING JIANG AND MLADEN EIC*

Department of Chemical Engineering, University of New Brunswick, P.O. Box 4400, Fredericton, New Brunswick E3B 5A3, Canada

meic@unb.ca

Abstract. Transport properties of ethane, butane and their binary mixtures in large crystals of silicalite-1, ZSM-5, and an MFI-zeolite membrane as well as agglomerates (pellets) of silicalite zeolites have been investigated by the Zero Length Column (ZLC) method. It was found that in the large crystals of silicalite-1 and ZSM-5, and in the membrane sample desorption of iso-butane was controlled by micropore diffusion, while in the case of pelleted silicalite sample it was controlled by macropore diffusion. The effective thickness of the zeolite membrane can be reasonably evaluated by comparing the diffusivity data obtained from the ZLC and gas permeation measurements. Desorption of ethane and n-butane in the large crystals of silicalite-1 and ZSM-5 and the membrane sample is attributed to both equilibrium effects and micropore diffusion. The diffusivity of ethane is significantly reduced in the presence of iso-butane giving rise to a micropore diffusion-controlled process. Furthermore, diffusion of iso-butane in the zeolite samples is affected by the counter flow of ethane.

Keywords: ethane, butane, ZLC method, diffusion, MFI-zeolites

1. Introduction

Research on diffusion involving zeolites has been mainly focused on single-component systems, although most practical applications of zeolites involve binary or multi-component diffusion. PFG NMR technique has been successfully used to study binary mixture systems (Snurr and Kärger, 1997; Jöst et al., 1998; Nivarthi and McCormick, 1995). However, this technique is limited to highly mobile species. The diffusivities of sterically hindered molecules (such as iso-butane) in zeolites are generally too small to be measured by NMR technique. Zero Length Column (ZLC) has been considered as a promising method. Counter-current diffusion of binary mixtures consisting of p-xylene/benzene and p-xylene/o-xylene in silicalite was investigated by the ZLC method using Stefan-Maxwell model to analyze experimental data (Brandani et al., 2000). However, in general very limited litera-

ture data have been so far available for binary mixture systems.

Zeolites of MFI type (e.g., silicalite and ZSM-5) possess channels defined by 10-membered oxygen rings with a diameter of ~ 0.55 nm, which can be used to separate gases on a scale of molecular sieving. Therefore, they have been considered as good candidates for inorganic membrane materials. These materials have been attracting considerable interest because of their mechanical strength, thermal stability and organic solvent resistance. Among the zeolite membranes studied so far, MFI-zeolite membranes supported on alumina or stainless steel have exhibited most reproducible permeance data. In a previous work (Ciavarella et al., 2000), permeation of gases (H_2 and/or butane) through a composite alumina-MFI-zeolite membrane has been reported. It was concluded that transport in the membrane was controlled by a composite zeolite-alumina layer formed at outer surface of the support, viz., zeolite based membrane behaves as a molecular sieve. From this point of view, the diffusion properties of sorbates

*To whom correspondence should be addressed.

in the zeolite pores play an important role in controlling gas permeation and determining separation efficiency of membrane materials.

In the present work, the diffusion of single components as well as binary mixtures of ethane, n-butane and iso-butane in large crystals of silicalite-1 and ZSM-5 zeolites, as well as a composite alumina-MFI zeolite membrane sample, and silicalite pellets have been investigated using the ZLC method. The diffusivity data obtained for the MFI zeolite crystals (silicalite and ZSM-5) and MFI-membrane have been compared and interpreted. The effects of counter sorbate species on the mobility of diffusing species have been explored in the co- and counter-current modes of operation.

2. Experimental

Silicalite-1 and NaH-ZSM-5 (denoted as ZSM-5 in the text) were synthesized by standard method (Zikanova and Derewinski, 1995). The distribution of crystal sizes was uniform with the dimensions, estimated from scanning electron micrographs (SEM), of $113 \times 20 \times 20$ and $14 \times 11 \times 8 \mu\text{m}$ for silicalite-1 and ZSM-5, respectively. These sizes correspond to the equivalent radii (R) of 22.1 and $6.7 \mu\text{m}$ respectively when the crystals are approximated as spheres. Silicalite pellets with average radii of 50, 390 and $550 \mu\text{m}$ were prepared by sieving the crashed commercial granules obtained from UOP Corporation. The zeolite samples were calcined at 550°C for 6 h to remove contaminants and organic templates before loading on the ZLC column.

The preparation of composite alumina-MFI membrane sample has been described in detail elsewhere (Moueddeb et al., in press; Ramsay et al., 1994; Piera et al., 1998). The macroporous alumina was supplied by SCT/US Filter (Membralox T1-70). The precursor was a clear solution of tetrapropylammonium hydroxide (TPAOH, 1 M solution from Aldrich) and silica (aerosil Degussa 380). A single-step synthesis protocol was employed in the preparation of the membrane (Ciavarella et al., 2000; Ramsay et al., 1994; Piera et al., 1998). The membrane sample used for the ZLC measurements was taken from the membrane tube by using a very hard and sharp knife to enable scraping of the surface that contains active zeolite layer.

Diffusion of single components and binary mixtures of ethane and butane was measured by the ZLC method. A very small amount of sample (less than 2 mg) was loaded into the ZLC column and activated at 270°C overnight to remove water present in the orig-

inal sample. The column was then equilibrated with a sorbate either as a single component or as binary mixture (for co-current diffusion measurements) diluted in a helium flow. The concentration of the sorbates was adjusted and maintained at a low level, or within linear region of adsorption isotherm as required by the ZLC theory. Desorption was carried out by purging with ultra-pure helium (for single-component and co-current diffusion measurements) or using helium plus counter sorbate (for counter-current diffusion measurements). The relative concentrations (c/c_0) of the effluent species from the ZLC column were measured on an on-line quadrupole mass spectrometer (Dycor Dymaxion, Ametek, USA) by monitoring the mass signals of 30 (C_2H_6^+ fragment) for ethane and 43 (C_3H_7^+ fragment) for butane species.

Detailed analysis of the ZLC curves for single-component diffusion has been described elsewhere (Eić and Ruthven, 1988). For a linear system with uniform spherical particles with a radius of R the relative effluent concentration (c/c_0) versus time (t) is given by:

$$\frac{c}{c_0} = \sum_{n=1}^{\infty} \frac{2L}{[\beta_n^2 + L(L-1)]} \exp(-\beta_n^2 Dt/R^2) \quad (1)$$

where D is the diffusivity and β_n 's are the eigenvalues given by the roots of auxiliary equation:

$$\beta_n \cot \beta_n + L - 1 = 0 \quad (2)$$

and

$$L = \frac{1}{3} \frac{\varepsilon v}{(1-\varepsilon)z} \frac{R^2}{K_H D} = \frac{1}{3} \frac{\text{purge flow rate}}{\text{crystal volume}} \frac{R^2}{K_H D} \quad (3)$$

where ε is the void fraction of particle layer, v interstitial gas velocity, z the ZLC bed depth, and K_H dimensionless Henry Law constant.

In the long time region the higher order terms in the summation can be ignored, and the function defined by Eq. (1) approaches asymptotic solution:

$$\frac{c}{c_0} = \frac{2L}{[\beta_1^2 + L(L-1)]} \exp(-\beta_1^2 Dt/R^2) \quad (4)$$

From Eq. (4), the values of L and D/R^2 can easily be determined from the slope and intercept of a plot of $\ln(c/c_0)$ versus time t .

The above analytical solution for single-component diffusion can be tentatively used for the evaluation of the co-current diffusion of binary mixtures at low concentrations. The theoretical analysis of ZLC curves for the counter-current diffusion requires further development of a theoretical model, which is a subject of our future study.

3. Results and Discussion

3.1. Diffusion of Single Components

The ZLC measurements were performed for the single-component systems involving ethane, n-butane and iso-butane in the temperature range of -40 to 0°C for ethane, and 0 to 140°C for butane depending on the samples. The concentration of the sorbate in helium was maintained between 0.025 and 0.06 vol% to maintain the system linearity. Helium purge flow rate varied from 40 to 120 cm^3 (STP) min^{-1} . As described above, the membrane sample was taken from the surface layer that also contains alumina support in addition to the zeolite crystals grown on the support. Therefore, pure alumina from the membrane support was a part of the sample used in the ZLC measurements. It was found that effects with respect to the diffusion through the alumina crystals were negligible, thus confirming the assumption that the effective diffusion through the membrane is completely controlled by intracrystalline diffusion involving the zeolite layer only. Representative ZLC curves for the diffusion of ethane, n-butane and iso-butane in the silicalite-1, ZSM-5 and membrane samples are displayed in Figs. 1–3. They are fitted by the ZLC model using Eqs. (1) and (2). Diffusivity data derived from the fitting results are summarized in Tables 1–3.

The reliable ZLC curves for ethane could only be obtained at much lower temperatures in comparison to butane. Although good tentative agreements between experimental data and the theory were obtained, e.g., Fig. 1(a), a close inspection of the ZLC curves for ethane shows that the appreciable initial drops in concentration corresponding to fast purging of the free volume of the system are not noticeable. This clearly indicates fast diffusion rates. Hufton and Ruthven (1993) have revealed that, when intracrystalline transport is fast compared to the rate at which sorbate is removed by the purge gas, the overall desorption process is controlled by equilibrium effect, and the corresponding ZLC curves can be extrapolated

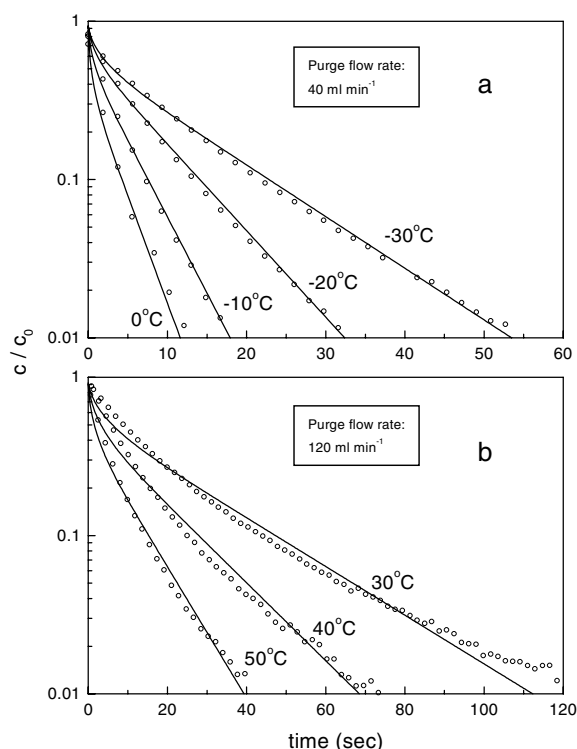


Figure 1. Experimental (symbols) and theoretical (solid lines) ZLC curves of ethane (a) and n-butane (b) in silicalite-1.

through the origin with a slope inversely proportional to Henry's constant. The rate of intracrystalline transport is determined by the size of sorbate molecule and the size of the zeolite crystals. In the present case, the kinetic size of ethane molecule is small relative to the micropores of the MFI zeolite and therefore the diffusion rate of ethane through the micropores may be comparable to its surface removal rate by the purge gas. In addition, the average size of the zeolite crystals in the samples (especially in the membrane) is small, which gives rise to a fast diffusion of ethane passing through the crystals. Therefore, the overall transport process of ethane in the samples seems to be attributed to both the intracrystalline diffusion and equilibrium-controlling effects. This conclusion is also confirmed by the rather small L values obtained from the theoretical fitting (see Tables 1 and 2). Compared to the membrane sample, the reliable ZLC curves for ethane in the ZSM-5 sample were only possible to obtain at lower temperatures, e.g., below -30°C , although the effective average size of the zeolite crystals in the membrane is much smaller than the size of the crystals in the ZSM-5. The relatively low transport rate

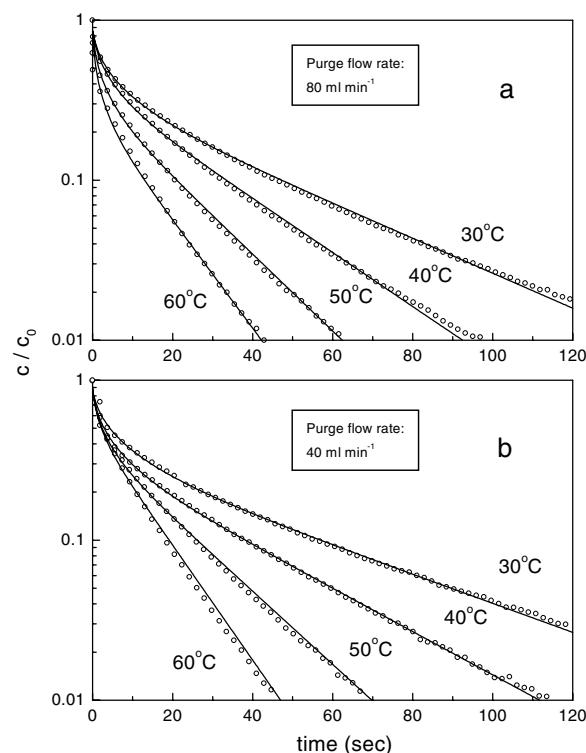


Figure 2. Experimental (symbols) and theoretical (solid lines) ZLC curves of iso-butane in silicalite-1 (a) and ZSM-5 (b).

of ethane in the membrane sample may result from the inhomogeneity of the zeolite material, and the possible effects of the surface barrier due to the existence of crystal defects in the membrane (*vide infra*).

Inspection of the ZLC curves of *n*-butane in the silicalite-1, ZSM-5 and membrane samples also reveals that the decrease in $\ln(c/c_0)$ appears to be nearly linear with time from the beginning of the process, suggesting that the desorption process is equilibrium-controlled (see Figs. 1(b) and 3(a)). For that reason the theoretical analysis of the ZLC curves is difficult. Obtained L values for *n*-butane diffusion in the samples are rather small, indicating that the desorption rate is controlled by both internal diffusion and convection. At small L values, the diffusivities estimated from the ZLC curves are subject to a considerable uncertainty.

For the diffusion of iso-butane in the silicalite-1, ZSM-5 and membrane samples (Figs. 2 and 3), much more significant initial drops can be observed compared to the ZLC curves of ethane and *n*-butane. The L values larger than 5 are generally obtained from the theoretical fittings of the ZLC curves (see Tables 1 and 2) ($L = 5$ is considered a point of transition from an

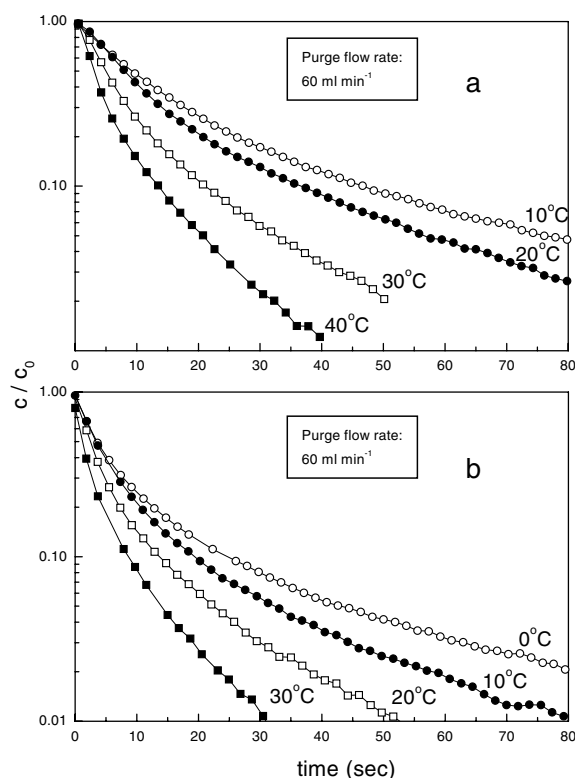


Figure 3. Experimental ZLC curves of *n*-butane (a) and iso-butane (b) in the membrane sample.

equilibrium-controlled to the intracrystalline diffusion process (Hufton and Ruthven, 1993)). The diffusivity values of iso-butane were confirmed from a series of measurements using different purge flow rates of helium. For instance, the values of D/R^2 for iso-butane in the membrane sample measured at 20°C at different purge flow rates (60–120 ml min⁻¹) vary only between 9.9 and 11.3 sec⁻¹ (Table 3). This indicates the validity of the simple theoretical ZLC model for the micropore diffusion-controlled process. Considering the equivalent radii of the silicalite-1 and ZSM-5 crystals (22.1 and 6.7 μm , respectively), the calculated absolute diffusivities for iso-butane are comparable to those obtained by Hufton and Ruthven (1993).

Millot et al. (Vlugt et al., 2000) studied the diffusion of *n*-butane and iso-butane in MFI-type zeolites using quasi-elastic neutron scattering technique. They reported that the diffusivities were significantly affected by the kinetic diameters of sorbate molecules. The diffusivity of iso-butane in ZSM-5 was found to be three orders of magnitude lower than *n*-butane because of the relatively larger kinetic diameter of iso-butane. In

Table 1. Diffusivity data for ethane, butane and their mixtures in the silicalite-1 sample.

Sorbate	Purge rate (ml min ⁻¹)	T (°C)	$D/R^2 \times 10^3$ (sec ⁻¹)	L
Ethane	40	-30	14.9	3.0
	40	-20	26.6	3.0
	40	-10	42.4	3.0
	40	0	47.3	5.0
n-Butane	120	30	6.8	3.0
	120	40	10.0	3.5
	120	50	15.5	4.2
Isobutane	80	30	4.9	6.3
	80	40	7.3	6.3
	80	50	9.0	9.0
	80	60	13.4	10.0
Ethane/isobutane (0.40)	40	0	19.4	7.0
	40	10	36.8	7.0
	40	30	66.7	7.0
Ethane/isobutane (0.08)	40	0	15.3	8.5
	40	10	20.0	10.0
	40	20	31.1	11.0
	40	30	42.5	12.0
Ethane/isobutane (0.04)	40	0	11.0	12.0
	40	10	16.9	12.0
	40	20	23.3	12.0
	40	30	35.6	12.0

contrast, our results are obviously in disagreement with the data of Millot et al. although the accuracy of the diffusion data for the n-butane remains unclear. The reason for the discrepancy is due to the different techniques used for the measurements of diffusion data. The ZLC method studies diffusion on a macroscopic scale, while the techniques such as neutron scattering study diffusion on a scale smaller than the crystallite size, which primary reveals microscopic features of molecular diffusion. Therefore, the results obtained from the ZLC method will be determined not only by the intracrystalline diffusion, but also by macroscopic crystal properties. Vlught et al. (Geier et al., 2001) used so-called transition path sampling method to investigate the diffusion of iso-butane in silicalite. In their study, they considered the effect of zeolite channel structure on the diffusivity. However, their computed diffusivity is more than one order of magnitude lower than most of the diffusion data reported in the literature. Furthermore, Geier et al. (Millot et al., 1999) considered the

Table 2. Diffusivity data for ethane and butane in the ZSM-5 sample.

Sorbate	Purge rate (ml min ⁻¹)	T (°C)	$D/R^2 \times 10^3$ (sec ⁻¹)	L
Ethane	120	-40	9.6	3.0
	120	-30	12.7	3.0
n-Butane	120	40	3.6	3.0
	120	60	6.0	3.0
	120	80	7.6	3.0
Isobutane	60	0	1.7	6.0
	60	20	3.0	6.0
	60	40	6.7	5.0
	60	60	11.8	5.0
Ethane/isobutane (0.40%)	80	-10	11.1	10.0
	80	0	24.4	6.5

effect of anisotropy of silicalite-1 on the diffusion of iso-butane. Interestingly, the diffusivity of iso-butane in silicalite obtained by averaging the effects in each direction (4×10^{-12} – 6×10^{-13} m² sec⁻¹) is very close to our results determined by the ZLC method and presented in Table 1 (vary between 2×10^{-12} and 6×10^{-12} m² sec⁻¹ depending on the temperature if the equivalent radius of the silicalite-1 is taken as 22.1 μm), confirming the reliability of the ZLC method.

Based on the diffusivity data obtained from ZLC measurements, Arrhenius plots of D/R^2 for the diffusion of iso-butane in the silicalite-1, ZSM-5 and membrane samples are shown in Fig 4. Good linear trends can be observed for the temperature range employed in the measurements. As indicated in Fig. 4, the activation energies derived from the plots for the silicalite-1

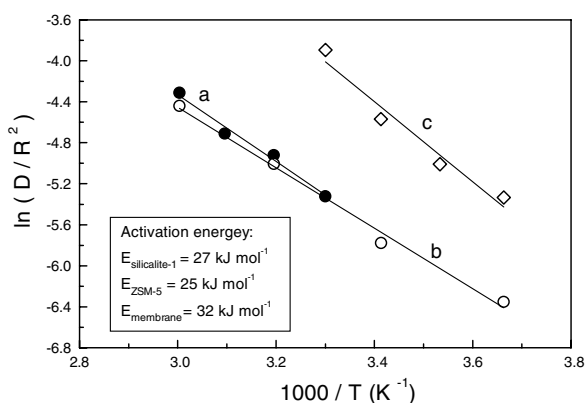


Figure 4. Arrhenius plots for the diffusion of iso-butane in the silicalite-1 (a), ZSM-5 (b) and membrane samples (c).

Table 3. Diffusivity data for butane and ethane in the membrane sample obtained from the gas permeation and ZLC measurements.

Sorbate	ZLC measurements				Gas permeation	
	Purge rate (ml min ⁻¹)	<i>T</i> (°C)	$D/R^2 \times 10^3$ (sec ⁻¹)	$D^\infty/R^2 \times 10^{-3}$ (sec ⁻¹)	$D^\infty/l \times 10^3$ (cm/s)	l/R^2 (μm ⁻¹)
Ethane	60	-40	28.8	3.0	20.7	0.50
	60	-30	44.6			
	60	-20	72.0			
n-Butane	60	10	3.5	0.9	6.7	0.14
	60	20	4.4			
	60	30	7.1			
	60	40	11.1			
Iso-butane	60	0	4.8	7.3	21.0	0.35
	60	10	6.7			
	60	20	10.4			
	60	30	20.3			
	90	20	9.9			
	120	20	11.3			

and ZSM-5 samples are very similar (~ 25 kJ mol⁻¹). This is not surprising since both silicalite and ZSM-5 are of the similar structure belonging to the MFI zeolites. However, for the membrane sample a relatively high activation energy (ca. 32 kJ mol⁻¹) was derived, which is in a good agreement with the results obtained by Millot et al. (34 kJ mol⁻¹) (Vlugt et al., 2000) and by Ciavarella et al. (2000) (31 kJ mol⁻¹) using gas-permeation techniques for the same type of membranes.

In order to obtain the diffusivity D , the equivalent radius of the zeolite crystals R has to be evaluated. For zeolites of uniform crystals, R values can be easily determined from their SEM images. For a composite zeolite membrane, however, the zeolite crystals in the membrane are not uniformly distributed. The internal structure of the membrane is composed of large alumina particles (between 20 and 30 μm). Small zeolite crystals are stacked on the surface of the larger alumina particles. Considering that the micropores of the zeolite control diffusion, it is most likely that only a dense layer of the zeolite membrane is involved in the process. The boundary of such a dense zeolite membrane cannot be visualized from the SEM image alone, which makes the determination of the thickness of the membrane difficult. Ratios of the pre-exponential factor of the diffusivity coefficient and effective membrane thickness (D^∞/l) can be readily obtained from gas permeation measurements. These ratios can then be compared with

D^∞/R^2 derived from the ZLC measurements (Jiang et al., 2001) in order to calculate values of l/R^2 . From these values the thickness of the membrane can be easily determined provided that the diffusivity data obtained from the ZLC and gas permeation measurements are comparable within the experimental errors. For n-butane, iso-butane and ethane, the values of l/R^2 listed in Table 3 vary between 0.14 and 0.5 μm⁻¹. Because of the uncertainty regarding diffusivity data for ethane and n-butane determined from the ZLC measurements as discussed above, only the l/R^2 value for iso-butane (ca. 0.4 μm⁻¹) should be considered for the estimate of l . Assuming that the equivalent radius R of the zeolite crystals in the membrane is about 3 μm (Moueddeb et al., in press; Ramsay et al., 1994; Piera et al., 1998), the calculated effective thickness of the membrane, l is about 4 μm, which corresponds to one or two layers of zeolite crystals. A similar effective membrane thickness has been reported earlier (Ciavarella et al., 2000). Here, one can ascertain that the effective thickness of the membrane for diffusion through the micropores of the zeolites is much smaller than the geometric thickness as observed from the SEM images.

The size of zeolite crystals is one of the most important factors in determining whether the transport process is micropore diffusion or equilibrium controlled. In the pelletized samples prepared from the commercial zeolites, the sizes of the zeolite crystals are very small. Therefore the diffusion of a sorbate through

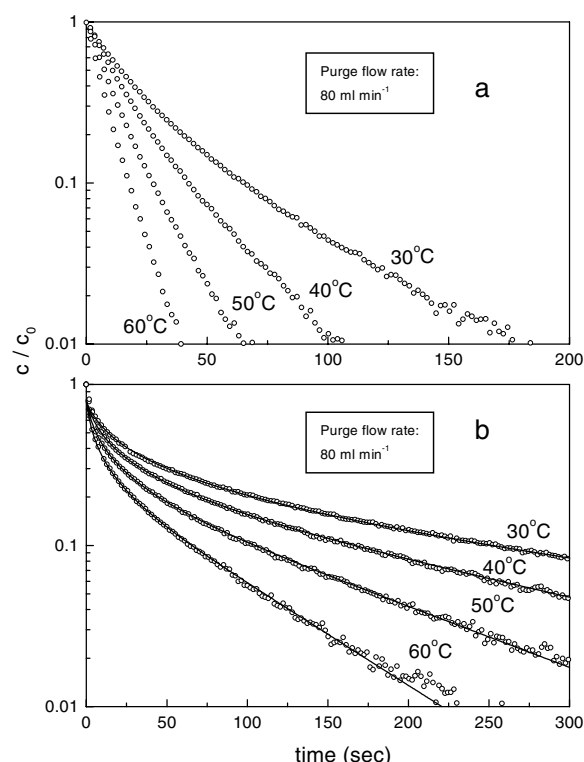


Figure 5. Experimental (symbols) and theoretical (solid lines) ZLC curves of iso-butane in pelletized silicalites with the particle radii of 50 (a) and 550 μm (b).

the intracrystalline medium may be much faster than the transport through the whole pellet, i.e., the transport process could be controlled by the macropores formed from stacking of the very small zeolite crystals or by equilibrium if the particle size of the pellets is small. Figure 5 shows the ZLC curves for iso-butane in the silicalite pellets with two different average particle sizes. As expected, in the case where the particles are of small size ($R = 50 \text{ mm}$) practically no initial drops are observed; the plots of $\ln(c/c_0)$ versus t are essentially linear, and can be extrapolated through the origin (Fig. 5(a)). It clearly indicates that the transport process is equilibrium-controlled. With the large particle size ($R = 550 \text{ mm}$), the macropore-controlled diffusion becomes dominant as indicated by the large initial drops in the plots of $\ln(c/c_0)$ versus t (Fig. 5(b)). Analysis of the ZLC curves for iso-butane in the pelletized silicalite samples using two larger particle sizes ($R_1 = 390$ and $R_2 = 550 \mu\text{m}$, see Table 4) shows that the L values derived from the fitting procedures are greater than 5, and with the ratios of the diffusional time constants ($D_{\text{eff}}/R^2\text{s}$) being close to the square ratio of the parti-

Table 4. Diffusivity data for iso-butane in the silicalite pellets.

T ($^{\circ}\text{C}$)	$D_{\text{eff}}/R_1^2 \times 10^3$ (sec^{-1})	$D_{\text{eff}}/R_2^2 \times 10^3$ (sec^{-1})	Ratio of D_{eff}/R^2
30	0.78	0.41	1.90
40	1.32	0.66	2.00
50	2.21	1.12	1.97
60	3.86	1.91	2.02

^aThe average R_1 and R_2 are 390 and 550 μm , respectively.

^b $6 \leq L \leq 10$.

cle radii R_2^2/R_1^2 (ca. 2.0), this analysis provides a clear proof of macropore-controlled diffusion process.

3.2. Diffusion in Binary Mixtures

The diffusion measurements involving binary mixtures were carried out in co- and counter-current modes monitored by mass spectroscopy.

Co-current ZLC curves for ethane mixed with iso-butane were measured using variable molar ratios of ethane/iso-butane. In order to avoid interference at the higher iso-butane concentrations (Jiang et al., 2002) the ZLC curves were measured at low total concentration in the gas phase, e.g. 0.06 vol%. The molar ratios of ethane/isobutane varied from 0.04 to 0.40. Figure 6 presents the experimental data (symbols) and the corresponding theoretical curves fitted by the ZLC model (solid lines) for the diffusion of ethane in the silicalite-1 sample in the presence of iso-butane. The diffusivity data derived from the fitting results are summarized in Table 1. Contrary to the ZLC curves for single-component system (Fig 1(a)), the reliable ZLC curves for ethane mixed with iso-butane can be obtained at much higher temperatures ($>0^{\circ}\text{C}$), indicating that the transport rate of ethane has been significantly reduced in the presence of iso-butane. This is also confirmed by the theoretically fitted diffusivities as shown in Table 1. Compared to single-component diffusion of ethane, much larger initial drops can be observed even at a very low concentration of iso-butane (Fig. 6). The L values derived from the theoretical fitting are greater than 7.0 (Table 1), indicating that the transport of ethane in the sample has been changed from a mainly equilibrium-control process to the micropore diffusion control. Similar results were also obtained with the ZSM-5 sample. In the absence of iso-butane, reliable ZLC curves were only obtained at temperatures below -30°C , while in the presence of iso-butane, they can be obtained at a temperature as high as -10°C (Table 2),

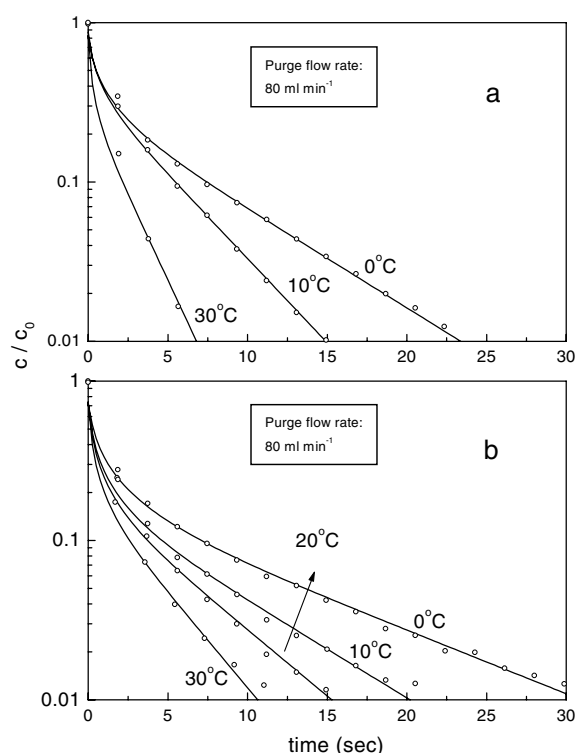


Figure 6. Experimental (symbols) and theoretical (solid lines) co-current ZLC curves of ethane in the presence of iso-butane in silicalite-1 with ratios of ethane to iso-butane of 0.40 (a) and 0.04 (b).

indicating that the presence of iso-butane decreases the rate of transport of ethane through the ZSM-5 samples.

Co-current ZLC curves of iso-butane in the presence of ethane were also measured. The concentration of ethane can be independently changed from 2 to 15%, since the mass signals of ethane do not interfere with the mass signal of isobutane at $m/e = 43$. However, at different concentrations of ethane, the obtained ZLC curves of iso-butane are very similar, and the derived diffusivity data show deviations of less than 15%, indicating that ethane has practically no effect on the diffusion of iso-butane in the co-current arrangement. This is not surprising even though one may expect that the presence of ethane could affect iso-butane diffusion. In the binary flux, a certain amount of iso-butane is replaced by the faster diffusing molecules, i.e., ethane consequently introducing additional concentration gradient of the second component. Based on that, diffusivity of the remaining iso-butane in the flux should be enhanced. However, this enhancement is considered insignificant due to much faster diffusion of ethane (much shorter retention time within the crystal

structure), thus rendering the difference in diffusivity very difficult to measure by the ZLC technique.

Attempts to measure the counter-current ZLC curves of ethane purged by helium plus iso-butane were not successful, because of the interference of the mass signal of $m/e = 30$ arising from iso-butane (Jiang et al., 2002). Therefore, only counter-current ZLC curves of iso-butane purged with helium containing ethane were obtained. The concentration of ethane in helium used as the counter purge varied from 0.25 and 10 vol%. Representative ZLC curves for iso-butane in the silicalite-1 crystals and silicalite pellets purged by ethane (1.0%) in helium at flow rates of 40 and 80 ml min⁻¹ are presented in Fig. 7. With the counter flow purge involving ethane/helium, the adsorbed iso-butane is quickly desorbed at the initial time, but the desorption curve levels off after certain time depending on the desorption temperature (see the separation marks shown on the curves in Fig. 7). Further increase in desorption time has a very limited effect on desorption of iso-butane. Compared with the co-current diffusion of binary mixture, the desorption rates of iso-butane are significantly reduced

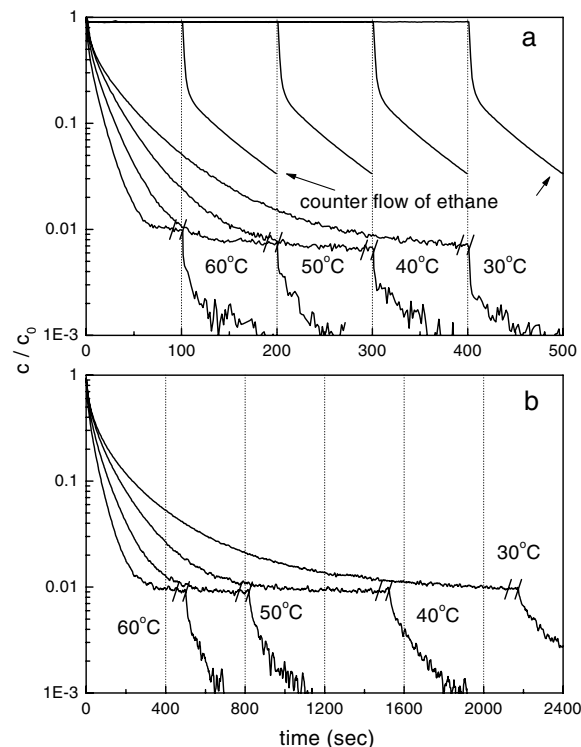


Figure 7. Counter-current diffusion of iso-butane purged by helium plus ethane in silicalite-1 (a) and silicalite pellets ($R = 390 \mu\text{m}$) (b).

by the counter flow of ethane/helium, indicating a strong interaction of the adsorbed iso-butane species with the ethane in the counter flow. As shown in Fig. 7(a), when the concentration of ethane in the counter flow decreases (see the inserted curves of counter flow of ethane), more iso-butane starts to desorb from the sample. This indicates that significant amount of iso-butane may be immobilized in the pores or channels of the zeolite in the presence of ethane in the counter-flow.

Kärger et al. (Snurr and Kärger, 1997; Jöst et al., 1998) have investigated diffusion properties of different binary mixture systems by using PFG NMR technique and revealed that the mobility of the faster diffusing species is in general reduced in the presence of a slower moving species, whereas the mobility of the slower moving species is not significantly affected by the faster diffusing species. However, the PFG NMR technique is usually limited to highly mobile species. The counter-current diffusion of p-xylene/benzene and p-xylene/o-xylene binary mixtures in silicalite has been investigated with the ZLC method and analyzed using the Stefan-Maxwell model by Brandani et al. (2000). They have drawn the same conclusion. In the present work, the results obtained from the co-current measurements of binary mixture of ethane/iso-butane clearly indicate that diffusion of faster species (ethane) is significantly reduced by slower species (iso-butane), which is consistent with the above-mentioned literature results. However, considering that the diffusivity of ethane is much higher than that of iso-butane, the former could be completely purged at the early stages of the desorption process leaving only the latter species in the zeolite. This would render diffusion of iso-butane mixed with ethane to be equivalent to the single component diffusion. Therefore, the effect of ethane upon the desorption of iso-butane cannot be elucidated from the co-current measurements. However, in the counter-current mode of diffusion measurements the iso-butane, which is pre-adsorbed in zeolite, will interact with ethane throughout the entire desorption process and therefore the effect of ethane upon the transport properties of iso-butane can be more evidently explained. Figure 7 clearly indicates that the diffusion of the slower moving species (iso-butane) is affected by the faster moving species (ethane). This is contrary to the results reported by Kärger et al. (Snurr and Kärger, 1997; Jöst et al., 1998) We have also obtained similar results involving the diffusion of n-butane affected by the counter flow of ethane in the silicalite-1 and ZSM-5 crystals and large

silicalite pellets (Jiang et al., 2002). The discrepancy between our observations and those reported in the literature needs a further investigation and clarification.

4. Conclusion

The transport properties of ethane, n-butane, iso-butane and their respective binary mixtures in MFI-type zeolite and membrane samples were investigated using the ZLC technique. It was found that the desorption process of ethane in the large crystals of silicalite-1 and ZSM-5 as well as the membrane sample is attributed to both micropore diffusion and equilibrium effects. The presence of iso-butane reduces the rate of intracrystalline transport of ethane in the large crystals, which gives rise to a micropore diffusion-controlled process. In the pelletized silicalite samples, the transport of ethane is mainly controlled by the equilibrium effect. Transport of iso-butane in the large crystals of silicalite-1 and ZSM-5 and the membrane sample is micropore diffusion-controlled, while that of iso-butane in the pelletized silicalite samples can be either equilibrium- or macropore diffusion-controlled depending on the particle size of the pellets. By comparing the results obtained from the ZLC and gas permeation experiments, the effective thickness of the membrane for gas permeation and separation has been estimated to be about one or two layers of zeolites. In the large crystals of silicalite-1 and ZSM-5 and the pelletized silicalite samples, diffusion of iso-butane is affected by the counter flow of ethane. Certain amount of iso-butane seems to be immobilized in the samples by interacting with ethane and can be released only when the concentration of ethane in the counter flow is decreased.

Acknowledgments

Financial supports for this project from NSERC (Canadian government) and ESTAC (Canadian chemical industry alliance) are gratefully acknowledged.

This paper is dedicated to Prof. Douglas M. Ruthven who pioneered the ZLC method with one of the co-authors of this paper (Mladen Eić).

References

- Brandani, S., M. Jama, and D.M. Ruthven, *Ind. Eng. Chem. Res.*, **39**, 821 (2000).

- Ciavarella, P., H. Moueddeb, S. Miachon, K. Fiaty, and J.A. Dalmon, *Catalysis Today*, **56**, 253 (2000).
- Eić, M. and D.M. Ruthven, *Zeolites*, **8**, 40 (1988).
- Geier, O., S. Vasenkov, E. Lehman, J. Kaerger, U. Schemmert, R.A. Rakoczy, and J. Weitkamp, *J. Phys. Chem.*, **105**, 10217 (2001).
- Huften, J.R. and D.M. Ruthven, *Ind. Eng. Chem. Res.*, **32**, 2379 (1993).
- Jiang, M., M. Eić, S. Miachon, J.A. Dalmon, and M. Kočirik, *Separation and Purification Technology*, **25**, 287 (2001).
- Jiang, M., M. Eić, and D.M. Ruthven, in *Fundamentals of Adsorption 7 (IAS)*, K. Kaneko, H. Kanoh, and Y. Hanzawa (Eds.), p. 732. IK International, Chiba-City, Japan, 2002.
- Jöst, S., N.K. Bär, S. Fritzsche, R. Haberlandt, and J. Kärger, *J. Phys. Chem. B*, **102**, 6375 (1998).
- Millot, B., A. Methivier, H. Jobic, H. Moueddeb, and M. Bee, *J. Phys. Chem.*, **103**, 1096 (1999).
- Moueddeb, H., P. Ciavarella, S. Miachon, and J.A. Dalmon, *Catalysis Today*, **67**, 177 (2001).
- Nivarthi, S.S. and A.V. McCormick, *J. Phys. Chem.*, **99**, 4661 (1995).
- Piera, E., A.G. Fendler, J.A. Dalmon, H. Moueddeb, J. Coronas, M. Mendez, and J. Santamaria, *J. Membr. Sci.*, **142**, 97 (1998).
- Ramsay, J., A.G. Fendler, A. Julbe, and J.A. Dalmon, French Patent No. 005652 (1994).
- Snurr, R.Q. and J. Kärger, *J. Phys. Chem. B*, **101**, 6469 (1997).
- Vlugt, T.J.H., C. Dellago, and B. Smit, *J. Chem. Phys.*, **113**, 8791 (2000).
- Zikanova, A. and D. Derewinski, *Zeolites*, **15**, 148 (1995).